

Supplemental Information

Immobilized symmetrical bis-(NHC) palladium complex as a highly efficient and recyclable Suzuki-Miyaura catalyst in aerobic aqueous media

Tahshina Begum,[‡]a Manoj Mondal,[‡]a Manash Protim Borpuzari,^a

Rahul Kar,^a Golap Kalita,^c Pradip K. Gogoi*^a and Utpal Bora*^b

^a Department of Chemistry, Dibrugarh University, Dibrugarh 786004, Assam, India

^b Department of Chemical Sciences, Tezpur University, Tezpur 784028, Assam, India

^c Department of Frontier Materials, Nagoya Institute of Technology, Gokiso-cho, Showa-ku, Nagoya 466-8555, Japan

E-mail: dr.pradip54@gmail.com; utbora@yahoo.co.in; ubora@tezu.ernet.in

Contents

1. General Information	1
2. Characterization Data of the Catalyst	1-7
3. General Information about Catalytic Experiments	7
4. Comparison of Palladium Catalysts with Literature Reports	8-9
5. Characterization data of the isolated coupling product	9-11
6. References	11-12
7. Copies of ¹ H NMR spectra of isolated products	13-25

General Information

All chemicals were obtained commercially and used without further drying or purification. Fourier Transform Infrared (FT-IR) measurements were recorded in KBr or CHCl_3 on a Shimadzu Prestige-21 FT-IR spectrophotometer. N_2 adsorption/desorption isotherms were measured using Quantachrome Instrument, BOYNTON BEACH, FL 33426 at liquid N_2 temperature. The surface area of the samples was calculated according to the BET equation and pore size distribution was evaluated using BJH algorithm. ^1H spectra were recorded in CDCl_3 on a JEOL, JNM ECS NMR spectrometer operating at 400 MHz. Melting points of the isolated coupling products were determined using BUCHI B450 melting point apparatus. Palladium loading in the catalyst and its leaching after catalytic cycle was determined using inductively coupled plasma-atomic emission spectrometry (ICP-AES) on a Thermo Electron IRIS Intrepid II XSP DUO. The SEM analysis was done using “JEOL, JSM Model 6390 LV” model. Silica gel (60-120 mesh) was purchased from SRL Chemicals, India. 3-chloropropyltriethoxysilane (CPTES) was purchased from Sigma Aldrich. $\text{Pd}(\text{OAc})_2$ was purchased from Spectrochem Pvt. Ltd., India. Due to insolubility of the silica-supported NHC-Pd complex in common organic solvents, its structural investigations were limited only to its physicochemical properties, like FT-IR, XRD, SEM-EDX, ICP-AES, elemental mapping and N_2 -adsorption-desorption spectral data.

Characterization Data of the Catalyst

FT-IR Analysis

The FTIR spectra of the samples prepared are presented in fig S1. For the samples, the band around 1642 and 3440 cm^{-1} can be assigned for the $\nu_{\text{O-H}}$ stretching and bending vibrations of the adsorbed water. The absorption peaks around 805 and 1084 cm^{-1} were found due to Si-O-Si structure of silica framework. A characteristic band at 951 cm^{-1} was seen due to the silanol group of silica, but after functionalization with CPTES and imidazole, the intensity of this band for all the samples decreases or even disappears, indicating the formation of -Si-O- bond, which is formed by the reaction between silanol groups of silica with the $(\text{C}_2\text{H}_5\text{O})_3\text{Si}$ - group of CPTES. In comparison with the simple silica, the bands at 2980 and 2930 cm^{-1} for the sample $\text{NHC}@/\text{SiO}_2$ was due to C-H stretching of CPTES. Compared with the unfunctionalized silica

and NHC@SiO₂, the significant features of the spectrum of the Pd catalyst were the appearance of the peak at 3180 (sp² C-H stretching vibration of the imidazole moiety), 2820 (N-CH₂ stretching vibration) and 1574 cm⁻¹ (C-N and C=C vibrations of the imidazole ring), which indicates the definite attachment of the all materials. In the low frequency region, the band detected around 470 cm⁻¹ was assigned to Pd-C stretching frequency.

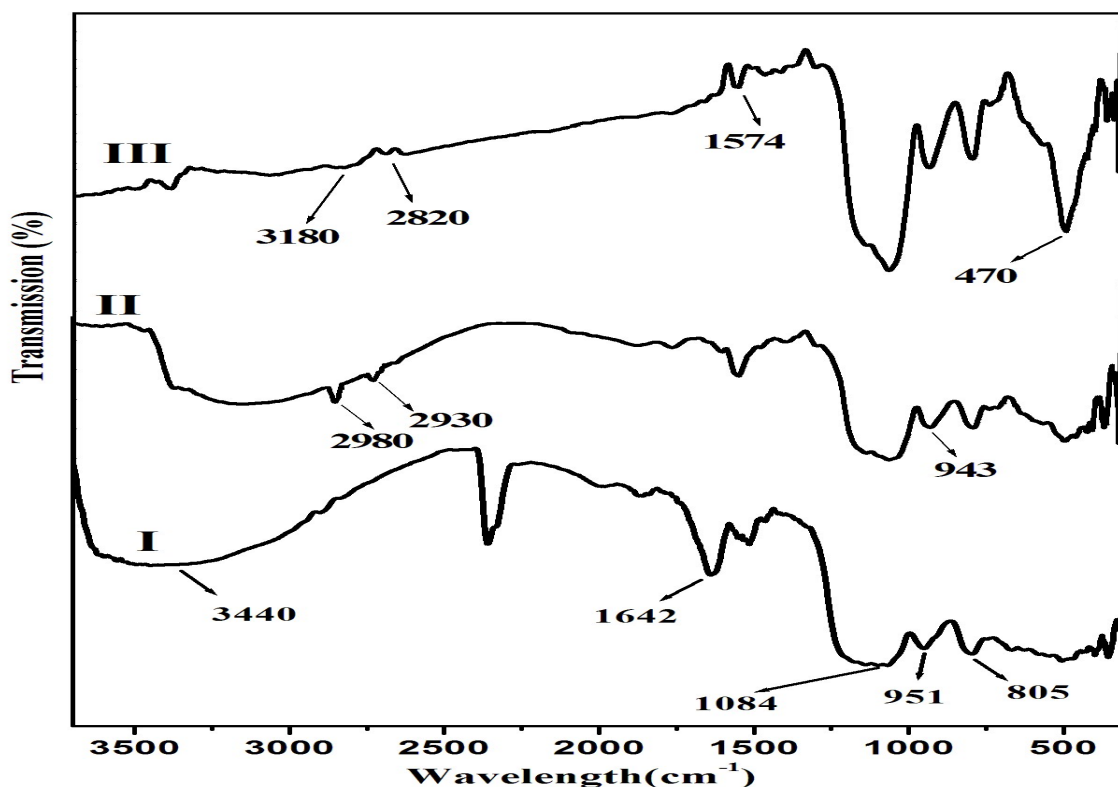


Figure S1: FTIR spectra: (I) Silica gel (SiO₂), (II) NHC@SiO₂, (III) Pd-NHC-CPTES@SiO₂

N₂ adsorption-desorption isotherm

The specific surface area and pore size distribution of the free silica, supported ligands and metal complex were determined by N₂ adsorption-desorption study. All the samples exhibited the type IV isotherm according to the IUPAC classification with a sharp hysteresis loop, which are characteristics of mesoporous materials (fig S2.) with highly uniform pore size distribution.

According to the BET measurements, the specific surface area and pore volume for the catalyst was 197.5 m²·g⁻¹ and 0.187 cm³·g⁻¹ respectively compared to parent silica (fig. S2). The structural parameters are summarised in the table (Table S1). A considerable decreased in the BET surface area and pore volume compared to the supported ligand indicates the immobilization of palladium on the silica matrix.

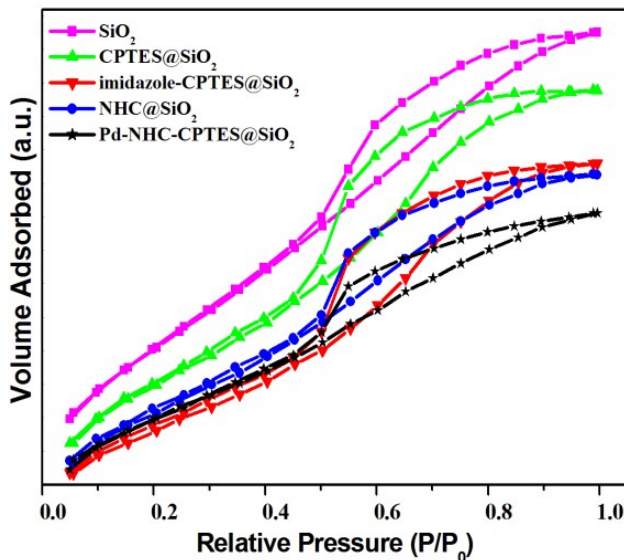


Figure S2: N₂ adsorption-desorption isotherm of the prepared samples

Table S1. Surface area and pore size distribution of the silica based samples

Entry	Sample	Surface area (m ² g ⁻¹)	Pore volume (cm ³ g ⁻¹)	Pore radius (nm)
1	SiO ₂	415.4	0.339	3.15
2	CPTES@ SiO ₂	353.2	0.251	3.02
3	Imidazole-CPTES@ SiO ₂	249.7	0.228	2.84
4	NHC@SiO ₂	204.3	0.207	2.47
5	Pd-NHC-CPTES@SiO ₂	197.5	0.187	2.12

XRD, SEM, EDS mapping, SEM-EDX and TEM analysis

The X-ray powder diffraction patterns of the silica and Pd(II) complex were shown in the fig S3, which are recorded over $2\theta = 15-60^\circ$. Both silica and Pd(II) complex shows a strong diffraction peak at low angles corresponding to $2\theta = 21.99^\circ$ (100), corroborate that the hexagonal mesoporous structure of silica remained roughly intact during the course of preparing the catalyst. An XRD spectrum of silica is highly ordered, showing two weak diffractions for the 110, 200 planes. No wide-angle XRD peak was observed in the spectra (fig S3 (b)) suggesting the absence of metallic palladium in the complex.

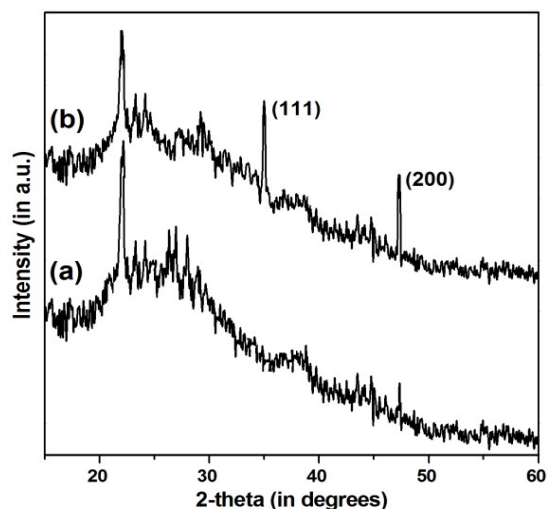


Figure S3: XRD pattern of (a) free silica, and (b) Pd-NHC-CPTES@SiO₂

The typical SEM images of the free silica and palladium complex clearly shows the morphological change which occurred on the surface of the silica matrix after loading of the metal. Fig. S4 shows the presence of palladium in the complex by indicating the decreasing particle size of silica matrix.

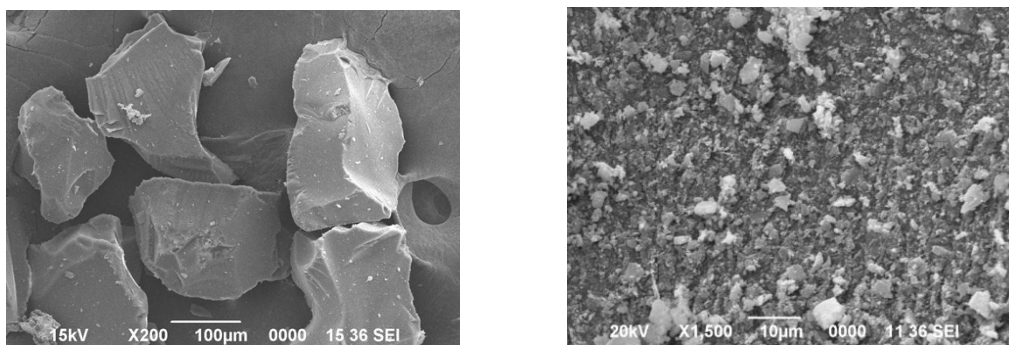


Figure S4: SEM image of (a) silica gel (SiO₂) (Figure copyright the Royal Society of Chemistry and reproduced with permission, Ref. 9), (b) Pd-NHC-CPTES@SiO₂

To further confirm the Pd-NHC-CPTES@SiO₂ structure, we take the elemental mapping by energy dispersive X-ray absorption spectroscopy (EDS). Fig. S5 shows that the distribution of palladium sites and silica is very uniform throughout the whole matrix.

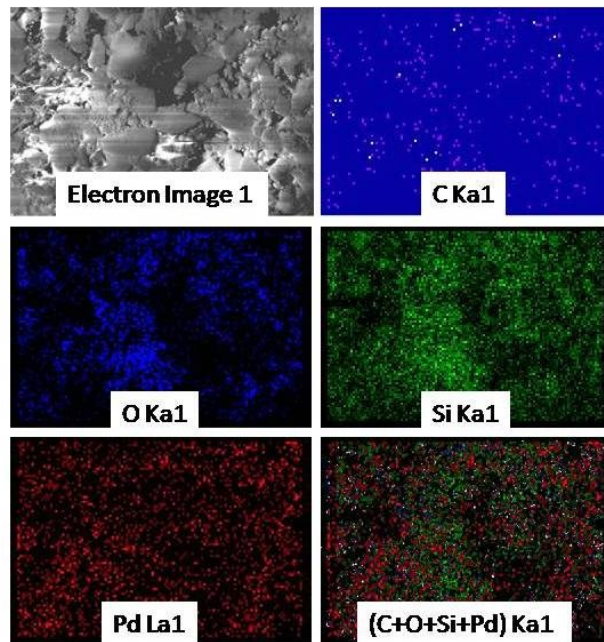


Figure S5: SEM image; EDS mapping of elements C, O, Si and Pd

TEM analysis showed that the size of the Pd particles had increased from 3-4 nm to 6-8 nm after sixth run (Fig S6).

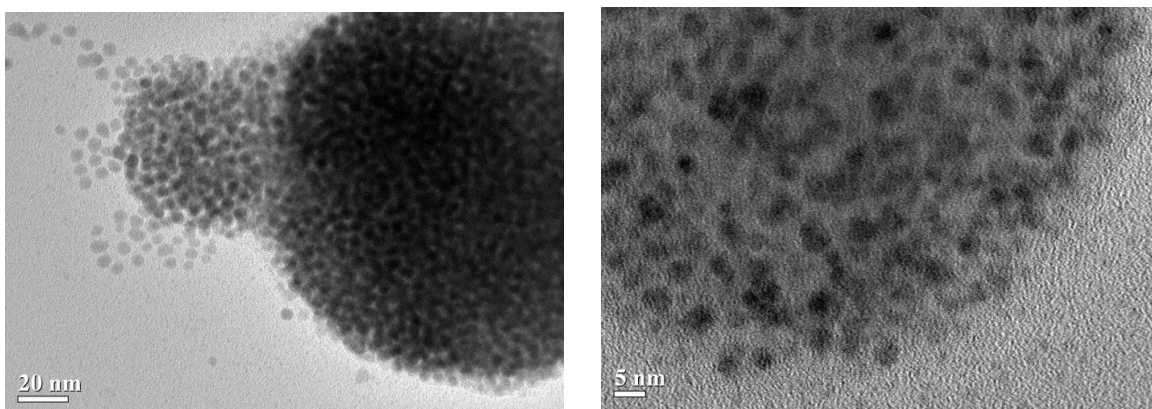


Figure S6: TEM images of fresh (left) and used catalyst (right)

The existence of palladium in the catalyst was confirmed by SEM-EDX analysis. EDX analysis of the metal complex shows the metal content along with the O and Si and suggests the formation of the metal with the anchored ligand at the various sites of the silica support (Fig. S6).

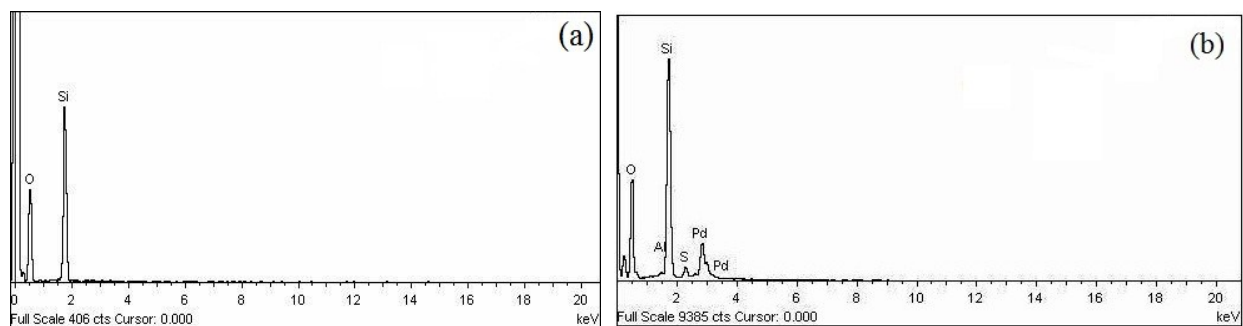


Figure S7: SEM-EDX spectra of (a) silica gel (SiO_2) (Figure copyright the Royal Society of Chemistry and reproduced with permission, Ref. 9), (b) Pd-NHC-CPTES@ SiO_2

The electronic properties of the Pd-NHC-CPTES@ SiO_2 complex was probed by X-ray photoelectron spectroscopy (XPS) analysis (**Figure S8**). The XPS spectrum of the Pd 3d core level region for the Pd-NHC-CPTES@ SiO_2 complex displays main peaks at 340.9 and 346.2 eV which can be attributed to the binding energy of Pd 3d_{5/2} and Pd 3d_{3/2}, respectively. These values correspond to the Pd(II) binding energies of the Pd-NHC-CPTES@ SiO_2 complex .

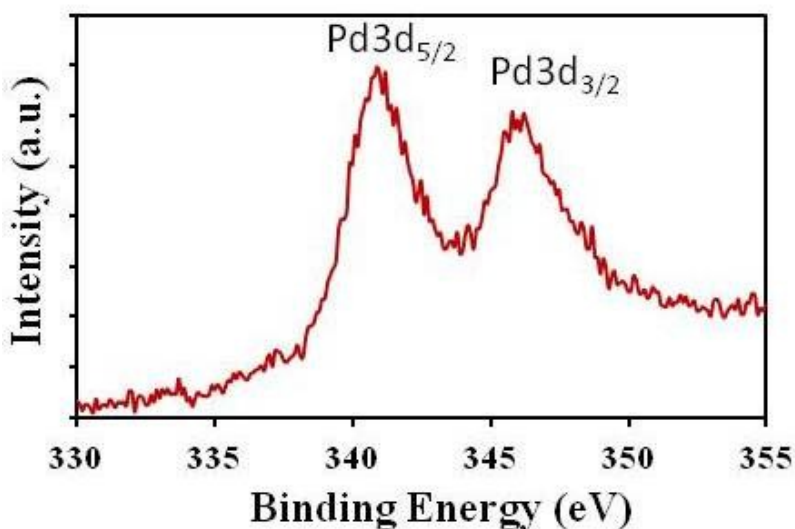


Figure S8: XPS spectra of the catalyst

To confirm the reduction of the Pd(II) to Pd(0) species XPS analysis of the catalyst (removed after 10 minute of reaction) was performed. **Figure S9** shows the high resolution XPS spectrum of the Pd 3d core in the catalytic mixture: four main peaks located at 343.0, 337.3 eV and 341.3, 335.9 eV were observed, which confirms that both Pd(II) and Pd(0) species are present during the first catalytic cycle, respectively. These results supports the reduction of Pd(II) to Pd(0) (catalyst pre-activation) under the experimental conditions.

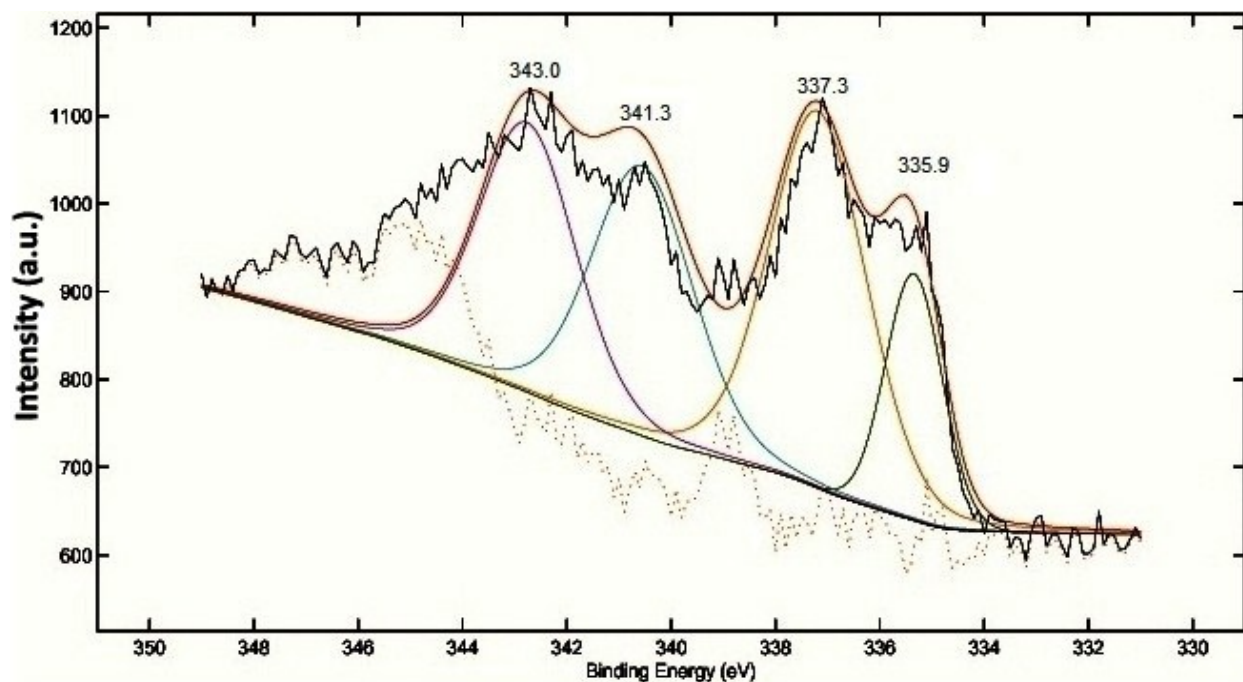


Figure S9: XPS spectra of the catalyst recovered from half done catalytic mixture
 The solid UV-Vis spectrum of Pd-NHC-CPTES@SiO₂ shows the presence of Pd(II) species. However, after completion of the reaction reduction of Pd(II) to Pd(0) was observed owing to the absence of the peak at 401 nm, which belongs to Pd(II) species (**Figure S10**).

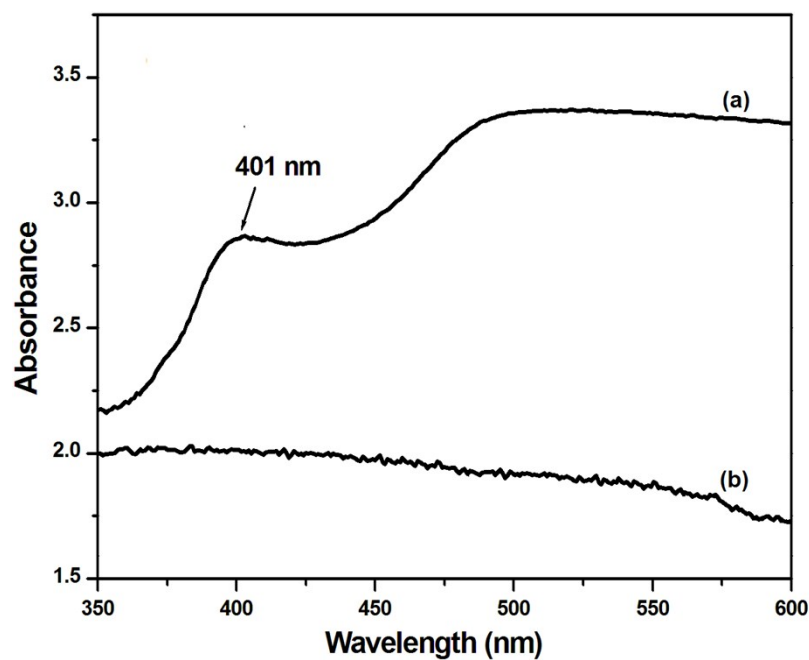


Figure S10: Solid UV-Visible spectra of Pd-NHC-CPTES@SiO₂ catalyst, (a) fresh and (b) after 1st catalytic cycle

General Information about Catalytic Experiments

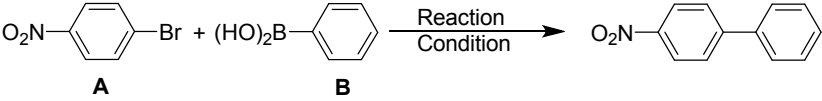
Cross-coupling reactions were carried out under aerobic conditions at temperature (50-80 °C). Progress of the coupling reactions was monitored using thin layer chromatography (TLC). The coupling products were isolated by column chromatographic using silica gel (60-120 mesh). The isolated products were confirmed by comparing the ¹H NMR spectral data with literature data.

Typical procedure for Suzuki-Miyaura coupling reaction

A 50 ml round-bottom flask was charged with a mixture of aryl halide (0.5 mmol), arylboronic acid (0.6 mmol), K₂CO₃ (1 mmol), required amount of catalyst (5 mg, 0.03 mol%Pd) and *i*PrOH/H₂O (4 mL). The mixture was stirred at given temperature for the indicated time. After completion, the reaction mixture was filtered and the residual solid was washed with the same solvent (3×5 mL). The resultant filtrate was diluted with brine (10 mL) and extracted with diethyl ether (3×10 mL), dried over anhydrous Na₂SO₄, and evaporated under vacuum. The crude residue was subjected to column chromatography (ethyl acetate-hexane, 0.5:9.5) to obtain the desired pure products.

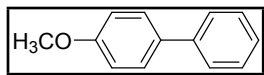
For recycling experiments, the residue catalyst was washed thoroughly with *i*PrOH/H₂O followed by ethyl acetate. After drying for overnight at 100 °C in an oven, the residual catalyst was subjected to subsequent run of the cross-coupling by charging with the required amount of substrates (aryl halide, arylboronic acid), K₂CO₃ and *i*PrOH/H₂O, without further addition of the catalyst.

Comparison of Palladium Catalysts with Literature Reports

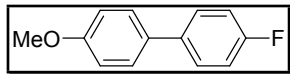
Table S2 Comparison of present methodology with other reported methods for Suzuki-Miyaura Cross-couplings						
						
Entry	Catalyst	Reaction Condition	Yield (%)	TON	TOF	Reference
1	SiO ₂ - <i>p</i> A-Cyan-Cys-Pd	Cat. (0.5 mol %), A(1.0 mmol), B (1.5 mmol), K ₂ CO ₃ , H ₂ O, 100° C, 5.5 h	91	182	33	1.
2	Polymer-supported macrocyclic Schiff base palladium complex	Cat. (0.1 mol %), A(1.0 mmol), B (1.5 mmol), K ₂ CO ₃ , DMF/H ₂ O, 25 °C, 20 min	99	990	2970	2.

3	Polymer anchored Pd(II) Schiff base Complex	Cat. (0.5 mol %), A(1.0 mmol), B (1.2 mmol), K ₂ CO ₃ , DMF/H ₂ O, 80 °C, 6 h	99	198	33	3.
4	NHC-Pd	Cat. (1 mol %), A(0.5 mmol), B (0.6 mmol), Na ₂ CO ₃ , DMF/H ₂ O, 50 °C, 6 h	94	94	15	4.
5	PS-Pd(II)-anthra	Cat. (0.5 mol %), A(1 mmol), B (1.2 mmol), K ₂ CO ₃ , DMF, air, 6 h	99	198	33	5.
6	[Gmim]Cl-Pd(II)	Cat. (0.1 mol %), A(1 mmol), B (1.2 mmol), Et ₃ N/[Aemim]Br, air, 2.5 h	90	900	360	6.
7	Polystyrene anchored Pd(II) azo complex	Cat. (0.5 mol %), A(1.0 mmol), B (1.5 mmol), K ₂ CO ₃ , H ₂ O, 70 °C, 6 h	98	196	32	7.
8	SMNPs-Salen Pd (II).	Cat. (0.5 mol %), A(1.0 mmol), B (1.5 mmol), K ₂ CO ₃ , DMF/H ₂ O, 100 °C, 3 h	96	192	64	8.
9	Pd@imine-SiO ₂	Cat. (0.463 mol %), A(0.5 mmol), B (0.6 mmol), Na ₂ CO ₃ , <i>i</i> PrOH/H ₂ O, r.t., 3 h	99	213	71	9.
10	Pd(PBIM)(OAc) ₂ @Nano-SiO ₂	Cat. (0.1 mol%), A (1 mmol), A (1.3 mmol), K ₂ CO ₃ , DMF/H ₂ O, 60 °C, 1 h	93	930	930	10.
11	Pd-NHC-CPTES@ SiO ₂	Cat. (0.03 mol %), A(0.5 mmol), B (0.6 mmol), K ₂ CO ₃ , <i>i</i> PrOH/H ₂ O, 50 °C, 40 min	98	3266	4948	Present work

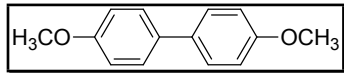
Characterization data of the product of the Suzuki-Miyaura reaction



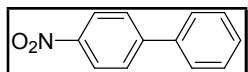
4-Methoxybiphenyl (Table 3, entry 1):¹¹ ¹H NMR (CDCl₃, 400 MHz, ppm) δ: 7.59-7.54 (m, 4H), 7.45-7.41 (m, 2H), 7.37-7.32 (m, 1H), 7.06-7.00 (m, 2H), 3.85 (s, 3H).



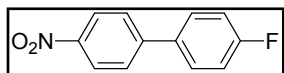
4-Fluoro-4'-methoxybiphenyl (Table 3, entry 2 and 17):¹¹ ¹H NMR (CDCl₃, 400 MHz, ppm) δ: 7.54-7.49 (m, 4H), 7.12-7.09 (m, 2H), 6.99-6.96 (m, 2H), 3.84 (s, 3H).



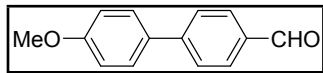
4, 4'-Dimethoxybiphenyl (Table 3, entries 3 and 15):¹¹ ¹H NMR (CDCl₃, 400 MHz, ppm) δ: 7.48-7.43 (m, 4H), 6.96-6.92 (m, 4H), 3.83 (s, 6H).



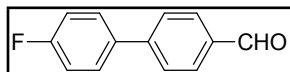
4-Nitrobiphenyl (Table 3, entry 4):¹¹ ¹H NMR (CDCl₃, 400 MHz, ppm) δ: 8.31-8.29 (m, 2H), 7.75-7.73 (m, 2H), 7.64-7.61 (m, 2H), 7.52-7.48 (m, 3H).



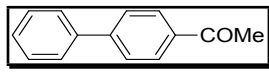
4-Fluoro-4'-nitro-biphenyl (Table 3, entry 5):¹¹ ¹H NMR (CDCl₃, 400 MHz, ppm) δ: 8.31-8.29 (m, 2H), 7.71-7.69 (m, 2H), 7.59-7.55 (m, 2H), 7.48-7.46(m, 2H).



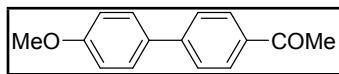
4'-Methoxy-[1,1'-biphenyl]-4-carbaldehyde (Table 3, entry 6):¹¹ ¹H NMR (CDCl₃, 400 MHz, ppm) δ: 10.03 (s, 1 H), 7.93-7.91 (m, 2H), 7.72-7.70 (m, 2H), 7.60-7.58 (m, 2H), 7.02-7.00 (m, 2H), 3.87 (s, 3H).



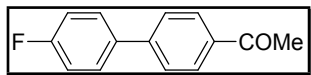
4-Formyl-4'-Flouro biphenyl (Table 3, entry 7):¹² ¹H NMR (CDCl₃, 400 MHz, ppm) δ: 10.05 (s, 1H), 7.98-7.96 (m, 2H), 7.92-7.90 (m, 2H), 7.61-7.56 (m, 2H), 7.21-7.16 (m, 2H).



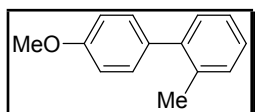
4-Acetyl biphenyl (Table 3, entry 8):¹¹ ¹H NMR (CDCl₃, 400 MHz, ppm, TMS) δ: 8.05-8.02 (m, 2H), 7.70-7.68 (m, 2H), 7.65-7.62 (m, 2H), 7.50-7.47 (m, 2H), 7.46-7.45 (m, 1H), 2.64 (s, 3H).



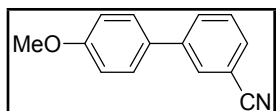
4-Acetyl-4'-methoxy biphenyl (Table 3, entry 9):¹¹ ¹H NMR (CDCl₃, 400 MHz, ppm) δ: 8.05-7.96 (m, 2H), 7.69-7.53 (m, 3H), 7.30-7.22 (m, 1H), 7.05-6.95 (m, 2H), 3.86 (s, 3H), 2.63 (s, 3H).



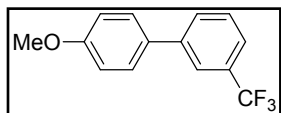
1-(4'-Flouro-[1,1'-biphenyl]-4-yl)ethanone (Table 3, entry 10): ¹H NMR (CDCl₃, 400 MHz, ppm) δ: 8.04-8.02 (m, 2H), 7.66-7.64 (m, 2H), 7.57-7.55 (m, 2H), 7.47-7.45 (m, 2H), 2.64 (s, 3H).



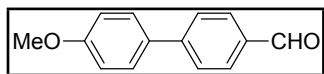
4'-methoxy-2-methyl-1,1'-biphenyl (Table 3, entry 11):¹³ ¹H NMR (CDCl₃, 500 MHz, ppm) δ: 7.25-7.14 (m, 6H), 7.94-7.91 (m, 2H), 3.80 (s, 3H), 2.26 (s, 3H).



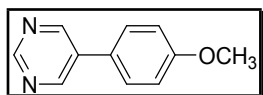
4'-methoxy-[1,1'-biphenyl]-3-carbonitrile (Table 3, entry 12): ¹H NMR (CDCl₃, 500 MHz, ppm) δ: 7.80 (d, *J*=1.5, 1H), 7.65 (d, *J*=1, 1H), 7.57-7.47 (m, 4H), 7.01-6.98 (m, 2H), 3.85 (s, 3H).



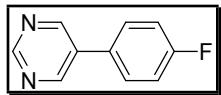
4'-methoxy-3-(trifluoromethyl)-1,1'-biphenyl (Table 3, entry 13): ¹H NMR (CDCl₃, 500 MHz, ppm) δ: 7.78 (s, 1H), 7.70-7.68 (d, *J*=7.5, 1H), 7.54-7.47 (m, 4H), 6.99-6.96 (m, 2H), 3.83 (s, 3H).



4'-Methoxy-[1,1'-biphenyl]-4-carbaldehyde (Table 3, entry 16):¹¹ ¹H NMR (CDCl₃, 400 MHz, ppm) δ: 10.03 (s, 1 H), 7.93-7.91 (m, 2H), 7.72-7.71(m, 2H), 7.60-7.59 (m, 2H), 7.04-7.00 (m, 2H), 3.87 (s, 3H).



5-(4'-Methoxyphenyl)pyrimidine (Table 3, entry 22):¹⁴ ¹H NMR (CDCl₃, 500 MHz, ppm) δ: 9.14 (s, 1H), 8.91 (s, 2H), 7.53-7.49 (m, 2H), 7.04-7.01 (m, 2H), 3.86 (s, 3H).



5-(4-Fluorophenyl)pyrimidine (Table 3, entry 23):¹⁴ ¹H NMR (CDCl₃, 500 MHz, ppm) δ : 9.18 (s, 1H), 8.89 (s, 2H), 7.55-7.51 (m, 2H), 7.21-7.17 (m, 2H).

References

1. M. Ghiaci, M. Zarghani, F. Moeinpour and A. Khojastehnezhad, *Appl. Organometal. Chem.*, 2014, **28**, 589.
2. Y. He and C. Cai, *Cat. Commun.*, 2011, **12**, 678.
3. S. M. Islam, P. Mondal, K. Tuhina, A. S. Roy, S. Mondal and D. Hossain, *J. Inorg. Organomet. Polym.*, 2010, **20**, 264.
4. J. H. Kim, J.W. Kim, M. Shokouhimehr, and Y. S. Lee, *J. Org. Chem.*, 2005, **70**, 6714.
5. M. Islam, P. Mondal, K. Tuhina, A. S. Roy, S. Mondal and D. Hossain, *J. Organom. Chem.*, 2010, **695**, 2284.
6. P. Karthikeyan, A. Vanitha, P. Radhika, K. Suresh and A. Sugumaran, *Tetrahedron Lett.*, 2013, **54**, 7193.
7. S. M. Islam, P. Mondal, A. S. Roy, S. Mondal and D. Hossain, *Tetrahedron Lett.*, 2010, **51**, 2067.
8. X. Jin, K. Zhang, J. Sun, J. Wang, Z. Dong and R. Li, *Cat. Commun.*, 2012, **26**, 199.
9. T. Begum, M. Mondal, P. K. Gogoi and U. Bora, *RSC Adv.*, 2015, **5**, 38085.
10. Z. Pahlevanneshan, M. Moghadam, V. Mirkhani, S. Tangestaninejad, I. Mohammadpoor-Baltork and H. Loghmani-Khouzani, *J. Organomet. Chem.*, 2016, **809**, 31.
11. W.-J. Zhou, K.-H. Wang, J.-X. Wang and Z.-R. Gao, *Tetrahedron*, 2010, **66**, 7633.
12. N. Kataoka, Q. Shelby, J. P. Stambuli and J. F. Hartwig, *J. Org. Chem.* 2002, **67**, 5553.
13. A. F. Littke, C. Dai and G. C. Fu, *J. Am. Chem. Soc.*, 2000, **122**, 4020.
14. Y. Kitamura, S. Sako, A. Tsutsui, Y. Monguchi, T. Maegawa, Y. Kitade and H. Sajiki, *Adv. Synth. Catal.* 2010, **352**, 718.

Copies of ¹H NMR spectra of isolated products

